

# Triaziflam and Diaminotriazine Derivatives Affect Enantioselectively Multiple Herbicide Target Sites

Klaus Grossmann<sup>a\*</sup>, Stefan Tresch<sup>a</sup> and Peter Plath<sup>b</sup>

<sup>a</sup> BASF Agricultural Center Limburgerhof, D-67114 Limburgerhof, Germany

<sup>b</sup> BASF Aktiengesellschaft, D-67056 Ludwigshafen, Germany

Fax 49621-60-27176. E-mail: Klaus.Grossmann@basf-ag.de

\* Author for correspondence and reprint requests

Z. Naturforsch. **56c**, 559–569 (2001); received April 19, 2001

Diaminotriazines, Cellulose Synthesis, Mitotic Disrupter Herbicides, Photosynthetic Electron Transport Inhibitors

Enantiomers of triaziflam and structurally related diaminotriazines were synthesized and their herbicidal mode of action was investigated. The compounds caused light and dark-dependent effects in multiple test systems including heterotrophic cleaver and photoautotrophic algal cell suspensions, the Hill reaction of isolated thylakoids and germinating cress seeds. Dose-response experiments revealed that the (*S*)-enantiomers of the compounds preferentially inhibited photosystem II electron transport (PET) and algae growth with efficacies similar to that of the herbicide atrazine. In contrast, the (*R*)-enantiomers of the diaminotriazines were up to 100 times more potent inhibitors of growth in cleaver cell suspensions and cress seedlings in the dark than the (*S*)-enantiomers. The most active compound, the (*R*)-enantiomer of triaziflam, inhibited shoot and root elongation of cress and maize seedlings at concentrations below 1  $\mu$ M. The meristematic root tips swelled into a club shape which is typical for the action of mitotic disrupter herbicides and cellulose biosynthesis inhibitors. Microscopic examination using histochemical techniques revealed that triaziflam (*R*)-enantiomer blocks cell division in maize root tips 4 h after treatment. The chromosomes proceeded to a condensed state of prometaphase but were unable to progress further in the mitotic cycle. Disruption of mitosis was accompanied by a loss of spindle and phragmoplast microtubule arrays. Concomitantly, cortical microtubules decreased which could lead to isodiametric cell growth and consequently to root swelling. In addition, a decline in cellulose deposition in cell walls was found 24 h after treatment. Compared to the (*R*)-form, triaziflam (*S*)-enantiomer was clearly less active. The results suggest that triaziflam and related diaminotriazines affect enantioselectively multiple sites of action which include PET inhibitory activity, mitotic disruption by inhibiting microtubule formation and inhibition of cellulose synthesis.

## Introduction

The herbicide atrazine (**8**, Table I) belongs to the class of 2,6-diamino-4-chloro-1,3,5-triazines which are inhibitors of photosystem II electron transport (PET) through binding to a specific site at the D1-protein (Fuerst and Norman, 1991). In the five decades since their discovery, many attempts have been initiated to synthesize new types of triazine derivatives with improved properties. Thirty years since the introduction of atrazine, triaziflam (**1**, Idetop<sup>®</sup>, Masahiro *et al.*, 1990) was commercialized for weed control in turf. The use of fluorinated alkyls in the 6-position of 1,3,5-tri-

azine (**9**) is known since 1974 (Cross and Feeny, 1974). In this context, 6-fluoroisopropyl seems to be more appropriate than 6-trifluoromethyl (**4**, **5**). In addition, the oxygen in the sidechain of triaziflam has been proved to be not essential for the herbicidal activity (**6**, **7**; Riebel *et al.*, 1999). Triaziflam (**1**) also contains a chiral C-atom in the sidechain. Omokawa and Konnai (1992) found different modes of action of enantiomers of  $\alpha$ -phenylethylamino-triazines (**10**, **11**). The (*S*)-isomers were potent inhibitors of PET, whereas the (*R*)-isomers suppressed root growth in the dark (Omokawa and Konnai, 1992; Omokawa *et al.*, 1994). However, studies on the mode of action of triaziflam and its enantiomers (**2**, **3**) have not been published in the standard herbicide literature so far. This also applies for the triaziflam analogues **4–7**.

Abbreviations: PET, photosystem II electron transport.

0939–5075/2001/0700–0559 \$ 06.00 © 2001 Verlag der Zeitschrift für Naturforschung, Tübingen · www.znaturforsch.com · D



Dieses Werk wurde im Jahr 2013 vom Verlag Zeitschrift für Naturforschung in Zusammenarbeit mit der Max-Planck-Gesellschaft zur Förderung der Wissenschaften e.V. digitalisiert und unter folgender Lizenz veröffentlicht: Creative Commons Namensnennung-Keine Bearbeitung 3.0 Deutschland Lizenz.

Zum 01.01.2015 ist eine Anpassung der Lizenzbedingungen (Entfall der Creative Commons Lizenzbedingung „Keine Bearbeitung“) beabsichtigt, um eine Nachnutzung auch im Rahmen zukünftiger wissenschaftlicher Nutzungsformen zu ermöglichen.

This work has been digitalized and published in 2013 by Verlag Zeitschrift für Naturforschung in cooperation with the Max Planck Society for the Advancement of Science under a Creative Commons Attribution-NoDerivs 3.0 Germany License.

On 01.01.2015 it is planned to change the License Conditions (the removal of the Creative Commons License condition “no derivative works”). This is to allow reuse in the area of future scientific usage.

Table I. Structures of diaminotriazines.

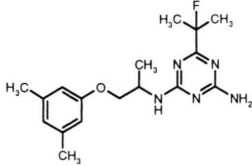
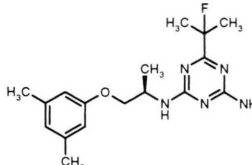
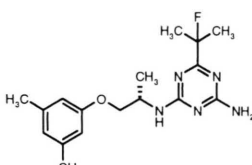
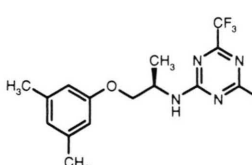
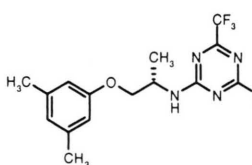
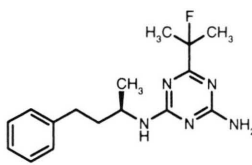
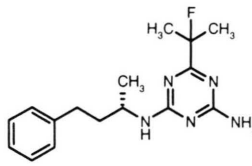
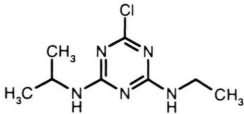
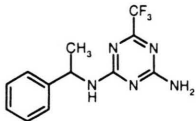
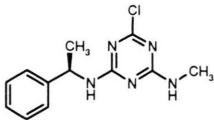
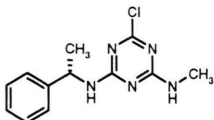
No.	Compound	CAS-Reg-No.	
1		131475-57-5	<i>N</i> <sup>2</sup> -[2-(3,5-dimethylphenoxy)-1-methylethyl]-6-(1-fluoro-1-methylethyl)-1,3,5-triazine-2,4-diamine <b>triaziflam</b> , Racemat (Masahiro <i>et al.</i> , 1990)
2		—	<i>N</i> <sup>2</sup> -[(1 <i>R</i> )-2-(3,5-dimethylphenoxy)-1-methylethyl]-6-(1-fluoro-1-methylethyl)-1,3,5-triazine-2,4-diamine
3		—	<i>N</i> <sup>2</sup> -[(1 <i>S</i> )-2-(3,5-dimethylphenoxy)-1-methylethyl]-6-(1-fluoro-1-methylethyl)-1,3,5-triazine-2,4-diamine
4		—	<i>N</i> <sup>2</sup> -[(1 <i>R</i> )-2-(3,5-dimethylphenoxy)-1-methylethyl]-6-(trifluoromethyl)-1,3,5-triazine-2,4-diamine
5		—	<i>N</i> <sup>2</sup> -[(1 <i>S</i> )-2-(3,5-dimethylphenoxy)-1-methylethyl]-6-(trifluoromethyl)-1,3,5-triazine-2,4-diamine
6		205531-86-8	<i>N</i> <sup>2</sup> -[(1 <i>R</i> )-1-methyl-3-phenylpropyl]-6-(1-fluoro-1-methylethyl)-1,3,5-triazine-2,4-diamine (Riebel <i>et al.</i> , 1998)
7		205531-85-7	<i>N</i> <sup>2</sup> -[(1 <i>S</i> )-1-methyl-3-phenylpropyl]-6-(1-fluoro-1-methylethyl)-1,3,5-triazine-2,4-diamine (Riebel <i>et al.</i> , 1998)

Table I. (cont.)

No.	Compound	CAS-Reg-No.	
8		1912-24-9	<b>Atrazine</b>
9		53387-85-2	Cross and Feeny, 1974
10		142275-63-6	6-Chloro- <i>N</i> <sup>2</sup> -methyl- <i>N</i> <sup>4</sup> -[(1 <i>R</i> )-1-phenylethyl]-1,3,5-triazine-2,4-diamine (Omokawa and Konnai, 1992)
11		142275-58-9	6-Chloro- <i>N</i> <sup>2</sup> -methyl- <i>N</i> <sup>4</sup> -[(1 <i>S</i> )-1-phenylethyl]-1,3,5-triazine-2,4-diamine (Omokawa and Konnai, 1992)

Therefore, we have synthesized these diaminotriazines to investigate their herbicidal mode of action using selected bioassays, the Hill reaction of isolated thylakoids and microscopic examination of changes in cell division processes.

## Materials and Methods

### Chemical synthesis

Synthesis of triaziflam (*R*)-enantiomer *N*<sup>2</sup>-[(1*R*)-2-(3,5-dimethylphenoxy)-1-methylethyl]-6-(1-fluoro-1-methylethyl)-1,3,5-triazine-2,4-diamine (**2**, Table I) started from (1*R*)-2-(3,5-dimethylphenoxy)-1-methylethylbiguanide hydrochloride (**A**, Fig. 1). The latter compound was pre-

pared in the following way. A solution of 26.9 g (0.15 mol) (2*R*)-1-(3,5-dimethylphenoxy)propan-2-amine in 150 ml 1,2-dichlorobenzene was saturated with gaseous HCl. After stirring for 1 h at 25 °C excess HCl was removed by bubbling dry nitrogen into the mixture. After adding 12.6 g (0.15 mol) *N*-cyanoguanidine, the suspension was heated to 145 °C and kept at this temperature for 4 h. After cooling to 25 °C, the solid was titrated with *tert*-butyl methyl ether and isolated (yield: 38 g (85%); Fp: 172 °C). Then, 10.8 g (0.06 mol) of 30% (w/w) methanolic NaOCH<sub>3</sub> was added dropwise at 0–5 °C to a suspension of 6 g (0.02 mol) of (1*R*)-2-(3,5-dimethylphenoxy)-1-methylethylbiguanide hydrochloride (**A**, Fig. 1) in 40 ml anhy-

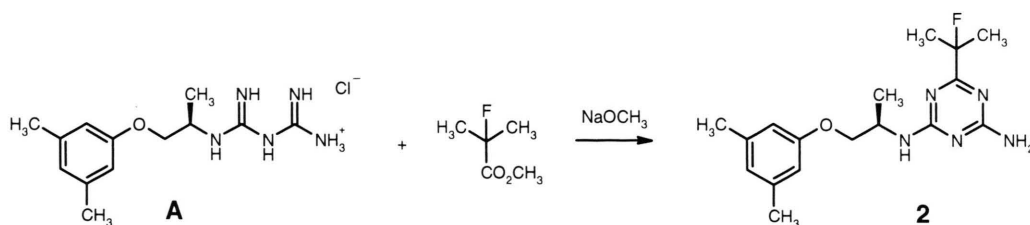


Fig. 1. Synthetic route to triaziflam enantiomers (**2**, **3**).

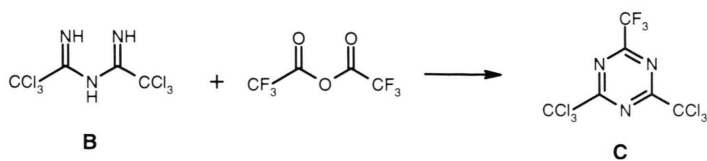


Fig. 2. Synthetic route to 2,4-bis(trichloromethyl)-6-(trifluoromethyl)-1,3,5-triazine (**C**).

drous methanol. While the mixture was kept at 0–5 °C, 7.2 g (0.06 mol) of methyl 2-fluoro-2-methylpropanoate was added dropwise. After stirring for 4 h at 25 °C, the mixture was heated to reflux for 6 h. Methanol was removed by distillation *in vacuo* and the residue was dissolved in ethyl acetate and washed with water. After drying over anhydrous sodium sulfate, the solvent was removed and the residue was purified by silica gel chromatography (eluent: *tert*-butyl methyl ether) yielding **2** (4.8 g, 72%) as an amorphous solid. The structure of **2** was determined by NMR.

Triaziflam (*S*)-enantiomer *N*<sup>2</sup>-[(1*S*)-2-(3,5-dimethylphenoxy)-1-methylethyl]-6-(1-fluoro-1-methylethyl)-1,3,5-triazine-2,4-diamine (**3**, Table I) was synthesized in an analogous manner (amorphous solid, yield: 57%).

Synthesis of compound **4**, *N*<sup>2</sup>-[(1*R*)-2-(3,5-dimethylphenoxy)-1-methylethyl]-6-(trifluoromethyl)-1,3,5-triazine-2,4-diamine, and **5** (Table I) started with known 2,4-bis(trichloromethyl)-6-(trifluoromethyl)-1,3,5-triazine (**C**) which resulted from the reaction of 2,2,2-trichloro-*N*-(2,2,2-trichloroethanimidoyl)ethanimidamide (**B**) with trifluoroacetic anhydride (Backer and Wanmaker, 1951; Fig. 2). Then, compound **C** reacted with (2*R*)-1-(3,5-dimethylphenoxy)propan-2-amine to

give *N*-[(1*R*)-2-(3,5-dimethylphenoxy)-1-methylethyl]-4-(trichloromethyl)-6-(trifluoromethyl)-1,3,5-triazin-2-amine (**D**) in 94% yield (Fig. 3). Subsequent ammonolysis of **D** yielded compound **4** (95%). In detail, compound **B** was synthesized by slowly adding 34 g (0.5 mol) of 25 % aqueous ammonia to 144.5 g (1 mol) of trichloroacetonitrile at 0 °C (Fig. 2). A white solid precipitated after 1 h of stirring at 0 °C. After additional stirring for 2 h, 500 ml of diethylether was added to obtain a solution. The organic phase was separated and dried over sodium sulfate. Evaporation of the ether at 5 °C resulted in a white solid (260.4 g, 85% yield; m.p. 30 °C). Compound **C** was prepared by adding 378 g (1.8 mol) trifluoroacetic anhydride dropwise to a solution of 260.4 g (0.85 mol) compound **B** in 200 ml toluene at 25 °C (Fig. 2). The reaction mixture was then heated to reflux for 5 h. Evaporation of toluene resulted in an oil which was distilled under reduced pressure: bp: 74–76 °C/0.3 mm. Yield: 280 g (86%). The product crystallized while standing. Compound **D** was synthesized by adding 3.58 g (20 mmol) (2*R*)-1-(3,5-dimethylphenoxy)propan-2-amine dropwise to a solution of 7.68 g (20 mmol) compound **C** in 75 ml THF at 25 °C (Fig. 3). After 16 h of stirring at 25 °C, the reaction was complete (tlc). THF was

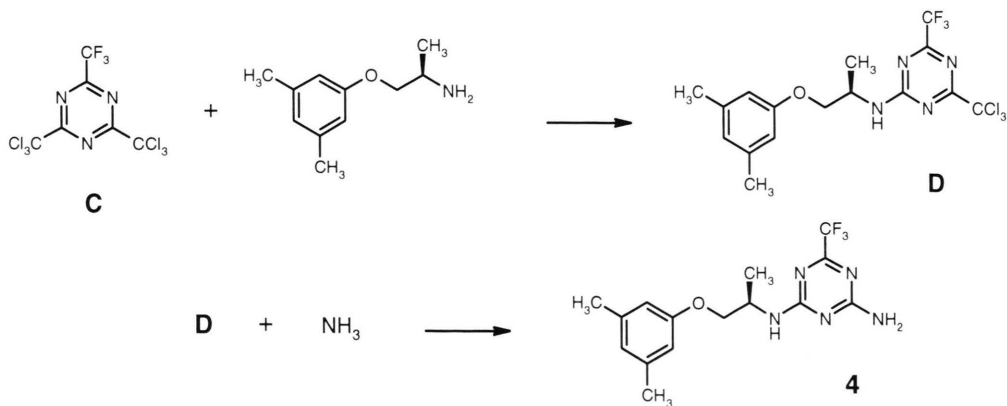


Fig. 3. Synthetic route from 2,4-bis(trichloromethyl)-6-(trifluoromethyl)-1,3,5-triazine (**C**) to 6-trifluoromethyl derivatives of triaziflam (**4**).



removed by distillation *in vacuo* and the residue was dissolved in 100 ml of hexane. The solution was washed with 5% HCl (1×) and water (3×). After drying over sodium sulfate hexane was removed by distillation. Oil, yield: 8.34 g (94%).

The following reaction resulted in compound **4** (Fig. 3). Here, 2.22 g (5 mmol) compound **D** were dissolved in 20 ml ammonia (20% w/w, in methanol) and stirred for 16 h at 25 °C. The methanol was removed and the residue re-dissolved in 50 ml diethylether. After washing with 10% aqueous citric acid and water, the organic phase was dried over sodium sulfate and evaporated (amorphous solid, yield: 1.62 g, 95%). In the same manner, *N*²-[(1*S*)-2-(3,5-dimethylphenoxy)-1-methylethyl]-6-(trifluoromethyl)-1,3,5-triazine-2,4-diamine (**5**) was prepared in 92% yield.

Compounds **6** and **7** (yield 53%) were prepared analogous to the procedure described for compounds **2** and **3** (Fig. 1). The enantiomers of 1-methyl-3-phenylpropylamine were synthesized according to Riebel *et al.* (1998).

Stock solutions of the chemical compounds in acetone were diluted 100-fold in the biological tests.

#### Algae bioassay

Cells of *Scenedesmus acutus* (Culture Collection Göttingen, 276-3a) were propagated photoautotrophically (Grossmann *et al.*, 1992). The bioassay was carried out in plastic microtitre dishes containing 24 wells (Grossmann *et al.*, 1992; Grossmann and Retzlaff, 1997). Before loading the wells with 0.5 ml cell suspension each, 0.5 ml medium and compound in acetone solution were added, allowing sufficient time for the organic solvent to volatilize. The 15 additional compartments between the wells were filled with sodium carbonate/bicarbonate buffer. The dishes were sealed with plastic lids and incubated on a shaker under continuous light at 23 °C. After 24 h, growth was measured photometrically.

#### Heterotrophic cell suspension bioassay

Freely suspended callus cells from *Galium mollugo* (DSM Collection of Plant Cell Cultures, Braunschweig, Germany) were cultivated in a modified Murashige-Skoog medium and the bioassay was performed as described previously (Gross-

mann *et al.*, 1992). The cells were subcultured at seven-day intervals. Acetone solutions of the compounds were pipetted into plastic tubes and the solvent allowed to evaporate before adding 2 ml of exponentially growing cell suspensions. The tubes (three replicates) were shaken at 400 rev min<sup>-1</sup> and 25 °C in the dark on a rotary shaker. After incubation for eight days, the conductivity of the medium was measured as the parameter for cell division growth (Grossmann *et al.*, 1992).

#### Hill reaction

Thylakoids were isolated from *Vicia faba* L. and effects on Hill reaction were studied as described by Münster *et al.* (1995) with modifications. Isolated thylakoids were suspended in reaction medium (0.75 ml) containing sucrose 0.1 M, tricine-NaOH (pH 8.0) *N*-[2-hydroxy-1,1-bis(hydroxymethyl)ethyl]glycine 50 mM, magnesium chloride 5 mM and chlorophyll 41 µg ml<sup>-1</sup>. The influence of the compounds on photosynthetic electron transport in photosystem II was performed according to the method of Avron and Shavit (1963). The assay mixture included thylakoid suspension (0.23 ml), test compound dissolved in 80% aqueous acetone (v/v, 0.05 ml), and K-ferricyanide (0.02 ml). During the subsequent illumination, ferrocyanide was formed in the Hill reaction. Then, in darkness, the ferrocyanide was allowed to react with ferric salt to form the ferrous salt which produced a complex with phenanthroline. The complex was measured photometrically at 510 nm.

#### Cress germination bioassay

Seeds of cress (*Lepidium sativum* L.) were placed in plastic Petri dishes (5 cm in diameter) filled with a vermiculite substrate. Stock solutions of the test compounds in acetone were added, together with 8 ml water (Grossmann and Retzlaff, 1997). Control seeds were moistened only with water and acetone. The dishes were incubated in a growth chamber at 25 °C in the dark for five days. Inhibition of germination and seedling development was evaluated visually (0 = no influence, 100 = total inhibition).

The results were expressed as percentage inhibition. Mean values of three replicates are given as the percentage inhibition relative to the control. Individual standard errors were less than 5%. All

experiments were repeated at least twice and proved to be reproducible. The results of a representative experiment are shown.

#### *Histochemical determinations*

Uniformly germinated seedlings of *Zea mays* (cv. Dea) with a root length of 3 cm were transferred into 50-ml glass vessels (1 seedling/vessel, 3 replications) in  $\frac{1}{2}$  strength Linsmaier-Skoog nutrient solution (light/dark: 16/8 h at 25/20 °C and 75% relative humidity, 250  $\mu\text{mol m}^{-2} \text{s}^{-1}$ , 400–700 nm; fluorescent lamps, Radium HRLV). After 15 h of adaptation, the compounds were added to the medium in acetone solution (0.1% final concentration of acetone). Controls received corresponding amounts of acetone alone, with no adverse effect on seedling growth. After 4 or 24 h of treatment, primary root tips of 5 mm length with meristematic and elongation zones were harvested. Then, root tips were fixed in 3.7% (v/v) formalin in phosphate buffered saline (PBS, pH 7.4) and embedded in paraffin as described (Ruzin, 1999). Longitudinal sections of 6  $\mu\text{m}$  thickness were obtained with a rotary microtome (Leica RM 2165, Bensheim, Germany).

Feulgen staining of sections for nucleic acids involved acid hydrolysis and aldehyde reaction with the fluorescent Schiff's reagent pararosanilin according to a standard protocol (Ruzin, 1999). Microscopic observation was on an Olympus BX51 epifluorescence microscope (Hamburg, Germany).

Specific staining for cellulose was based on a modified method described by Taylor *et al.* (1996). Root sections were deparaffinized and washed in phosphate-citrate buffer (pH 5.6) as described (Ruzin, 1999). The sections were then subjected to an enzymatic digestion of hemicelluloses and pectins through incubation in phosphate-citrate buffer containing 1% (w/v) pectinase and 2% (w/v) hemicellulase (Sigma, Deisenhofen, Germany) for 50 min at 37 °C. After washing in phosphate-citrate buffer and PBS, the samples were incubated in 100  $\mu\text{l}$  PBS containing 50  $\mu\text{g/ml}$  bacterial cellulose-binding domain conjugated to biotin (Sigma) for 1 h at room temperature. The domain was conjugated using a biotin-protein labeling kit as described (Molecular Probes Europe BV, Leiden, The Netherlands). The samples were

then treated with streptavidin-oregon green 488 (Molecular Probes) for 30 min, washed in PBS and mounted in a PBS/glycerol solution (1:1, v/v) for observation.

Microtubules were labeled with monoclonal antibody against polymerised  $\beta$ -tubulin (Sternberger Monoclonals, Lutherville, Maryland, USA), and followed by fluorescent Alexa 488-conjugated secondary antibody (Molecular Probes) using a modification of the method described (Ruzin, 1999; Eun *et al.*, 2000). First, root tips were fixed in 4% (w/v) paraformaldehyde in microtubule stabilising buffer (MSTB, pH 6.9) containing 60 mM PIPES (piperazine-N,N'-bis[2-ethanesulfonic acid]), 25 mM HEPES (N-2-hydroxyethylpiperazine-N'-2-ethanesulfonic acid), 10 mM EGTA (ethylene glycol-bis[ $\beta$ -aminoethylether]-N,N,N',N'-tetraacetic acid), 0.2 g/l  $\text{MgSO}_4 \times 6 \text{H}_2\text{O}$  for 3 h and then, frozen in liquid nitrogen. Longitudinal sections of 15  $\mu\text{m}$  thickness were obtained with a cryostat (Frigocut-2800 E, Reichert-Jung, Leica, Bensheim, Germany) and placed on slides coated with 3-aminopropyltriethoxysilane. Then, the slides were incubated in MSTB containing 1% (w/v) bovine serum albumin for 30 min at 37 °C. Incubation with tubulin antibodies and the secondary antibodies was carried out for 1 h, respectively, at 37 °C. The primary and secondary antibodies were diluted with PBS containing 1% (w/v) bovine serum albumin to 1:400 and 1:50, respectively. Nuclear DNA was stained with Hoechst 33342 (1  $\mu\text{g/ml}$ ) for 10 min (Eun *et al.*, 2000). The labeled slides were mounted with Pro-Long Antifade (Molecular Probes) for microscopic observation.

## **Results and Discussion**

### *Light-dependent effects*

As shown in Table II, the diaminotriazines (for structures see Table I and chemical synthesis Figures 1–3) effectively inhibited the Hill reaction for photosystem II electron transport (PET) using isolated thylakoids from *Vicia faba* with ferricyanide as electron acceptor. Based on the concentrations required for 50% inhibition ( $\text{IC}_{50}$ ), enantiomers of triaziflam (**2**, **3**) exhibited similar PET inhibitory activities. However, their activities were roughly 10 times lower than that of the reference PET inhibitor, atrazine. Enantiomers of a triaziflam de-

Table II. Inhibitory effects of diaminotriazines and atrazine on growth of green algae and on photosynthetic electron transport in photosystem II (Hill-reaction), germination of cress seeds and growth of heterotrophic cell suspensions of cleaver.

No.	Compounds	Algae	Molar concentration required for a 50% inhibition (IC <sub>50</sub> ) in:		
			Hill-reaction	Cress germination	Cell suspensions
Triaziflam					
1	Racemat	$8.4 \times 10^{-7}$	$3.0 \times 10^{-6}$	$4.1 \times 10^{-7}$	$1.5 \times 10^{-8}$
2	R-enantiomer	$9.0 \times 10^{-7}$	$4.5 \times 10^{-6}$	$5.1 \times 10^{-8}$	$7.0 \times 10^{-9}$
3	S-enantiomer	$7.0 \times 10^{-7}$	$3.5 \times 10^{-6}$	$4.1 \times 10^{-6}$	$1.9 \times 10^{-8}$
6-Trifluoromethyl-derivative					
4	R-enantiomer	$3.7 \times 10^{-7}$	$1.3 \times 10^{-6}$	$7.0 \times 10^{-6}$	$1.5 \times 10^{-8}$
5	S-enantiomer	$2.5 \times 10^{-7}$	$1.3 \times 10^{-6}$	$7.0 \times 10^{-5}$	$3.1 \times 10^{-7}$
Derivative without oxygen in the sidechain					
6	R-enantiomer	$3.1 \times 10^{-6}$	$3.7 \times 10^{-6}$	$3.5 \times 10^{-7}$	$5.8 \times 10^{-9}$
7	S-enantiomer	$2.8 \times 10^{-7}$	$4.0 \times 10^{-7}$	$3.5 \times 10^{-6}$	$1.0 \times 10^{-7}$
8	Atrazine	$3.4 \times 10^{-7}$	$3.5 \times 10^{-7}$	$\geq 10^{-4}$	$2.6 \times 10^{-5}$

rivative substituted with 6-trifluoromethyl on the triazine ring (**4**, **5**) also showed equivalent PET inhibitory activity, which was slightly higher than that of triaziflam (Table II). However, when enantiomers of a triaziflam analogue without oxygen in the sidechain (**6**, **7**) were compared, a notable chiral effect was observed (Table II). The PET inhibitory activity of the (*S*)-form (**7**) was found to be 10 times stronger than that of the (*R*)-form (**6**), and therefore nearly equivalent to that of atrazine (**8**). In general, the PET inhibitory activities of the diaminotriazines tested *in vitro* correlated with their effects on phototrophic growth in the green alga *Scenedesmus acutus* (Table II). This suggests that the influence of triaziflam and its derivatives on phototrophic growth is triggered through an inhibition of PET activity which appears to be similar to that of the conventional 1,3,5-triazine herbicide, atrazine.

#### Effects in darkness

However, in addition to the light-dependent effects and contrast to atrazine, the diaminotriazines showed strong preemergence activity on germinating seeds of cress in darkness (Table II). With increasing compound concentration, seedling development and elongation of hypocotyl and particularly roots were inhibited and both organs were swollen (Fig. 4). Concomitantly, the hypocotyl tis-

sue appeared glassy, while the root developed as brown. In the case of the (*R*)-isomer of triaziflam (**2**), root growth was completely inhibited at concentrations around 1  $\mu\text{M}$  (Fig. 4). In cress, these symptoms roughly resembled those caused by mitotic disrupter or cellulose-biosynthesis inhibiting herbicides. As reported by Omokawa *et al.* (1987), structurally related  $\alpha$ -substituted benzylamino-*s*-triazines exhibited phytotoxic properties distinct from those induced by atrazine, however, dependent on the respective enantiomer used (Omokawa and Konnai, 1992; Omokawa *et al.*, 1994). The (*S*)-isomers were potent inhibitors against PET, whereas the (*R*)-isomers showed growth regulating effects in the dark, including inhibition of shoot and root growth and secondary rhizome induction in *Cyperus serotinus* (Omokawa and Konnai, 1992; Omokawa *et al.*, 1994). The latter activity has been characterised as cytokinin-like (Omokawa *et al.*, 1994). In the cress germination test, the (*R*)-enantiomers of triaziflam and its derivatives were 100 (for triaziflam, **2**) and 10 times (for the derivatives; **4**, **6**) more active than the (*S*)-forms (**3**, **5**, **7**; Table II, Fig. 4). Similar results were obtained in heterotrophic suspension cultures of *Galium mollugo* (Table II). This system offers an appropriate model system for meristematic tissue, since growth is governed in both cases mainly by cell division activity and both cell species generally contain chloroplasts only as proplastids (Gross-

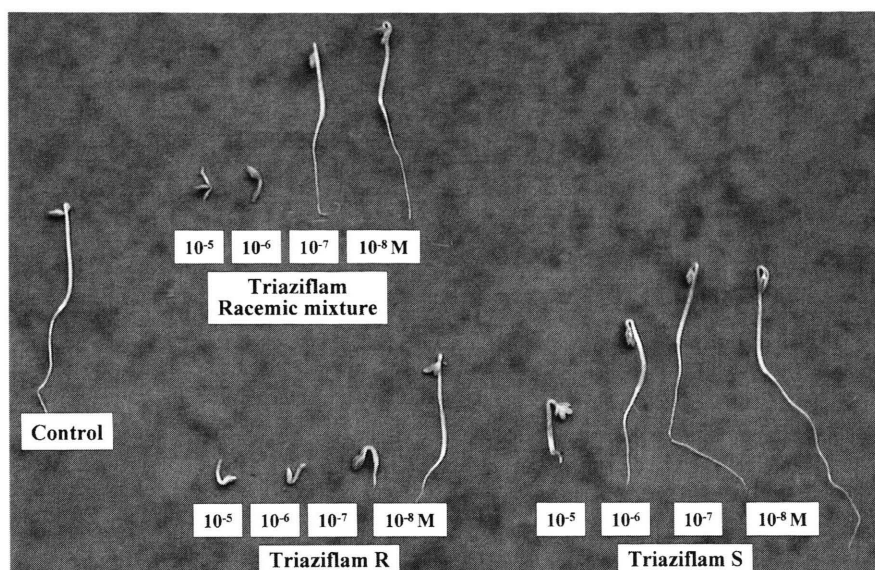


Fig. 4. Effects of triaziflam enantiomers (**2**, **3**) and racemate (**1**) on growth of cress seedlings in the dark.

mann *et al.*, 1992). As shown in Table II, cell division activity in *Galium* cell suspensions was particularly inhibited by the (*R*)-enantiomers of the diaminotriazines (**2**, **4**, **6**).

#### Histochemical observations

Histochemical methods based on specific reactions of dyes and molecular probes for nucleic acids,  $\beta$ -tubulin or cellulose were used to elucidate herbicide effects on cell division processes including mitosis and microtubule and cell wall formation in maize roots. Studies focused on the enantiomers of triaziflam, since these were the most potent compounds. Seedlings were treated with compounds for 4 and 24 h hydroponically. Although less potent than mitotic disrupter herbicides such as pendimethalin (Vaughn, 2000), compounds caused characteristic meristematic root tip swelling into a club shape and reduced root elongation (not shown). Tips of primary and adventitious roots were sampled and serial longitudinal sections were processed for fluorescence microscopic examination (Fig. 5). In order to examine compound effects on mitosis and microtubules, the Feulgen method was applied for nuclei and chromosome staining and microtubule arrays were visualized by means of monoclonal antibody against polymerized  $\beta$ -tubulin. After 4 h of treatment with

10  $\mu$ M of triaziflam (*R*)-enantiomer (**2**), cell division in the apical root meristem was completely blocked. The chromosomes proceeded to a condensed state of prometaphase, but were unable to progress further in the mitotic cycle (Fig. 5A). Cells at metaphase, anaphase and telophase were not found. After 24 h, nuclear membranes reformed around the chromosomes, resulting in strongly lobed nuclei and occasionally, in micronuclei distant from the main nucleus (not shown). Effects of triaziflam (*S*)-enantiomer (**3**) were less pronounced. At 4 h after treatment with 10  $\mu$ M, a few cells at metaphase or at later mitotic stages were present (Fig. 5A).

Treatment with 10  $\mu$ M triaziflam (*R*)-enantiomer (**2**) for 4 h affected all microtubule arrays in meristematic maize root cells (Fig. 5B). A decrease in cortical microtubules and a complete loss of preprophase band and organized arrays of spindle and phragmoplast were caused. Kinetochore microtubules were misorientated and co-localized with condensed chromosomes of prometaphase. Consequently, chromosomes cannot move to the poles of the cell during mitosis. In addition, loss of cortical microtubules were observed. This results in an increase in radial cell expansion and a concomitant decrease in elongation, which leads to the phenomenon of root clubbing in the zone of root elongation (Vaughn, 2000). The microtubule



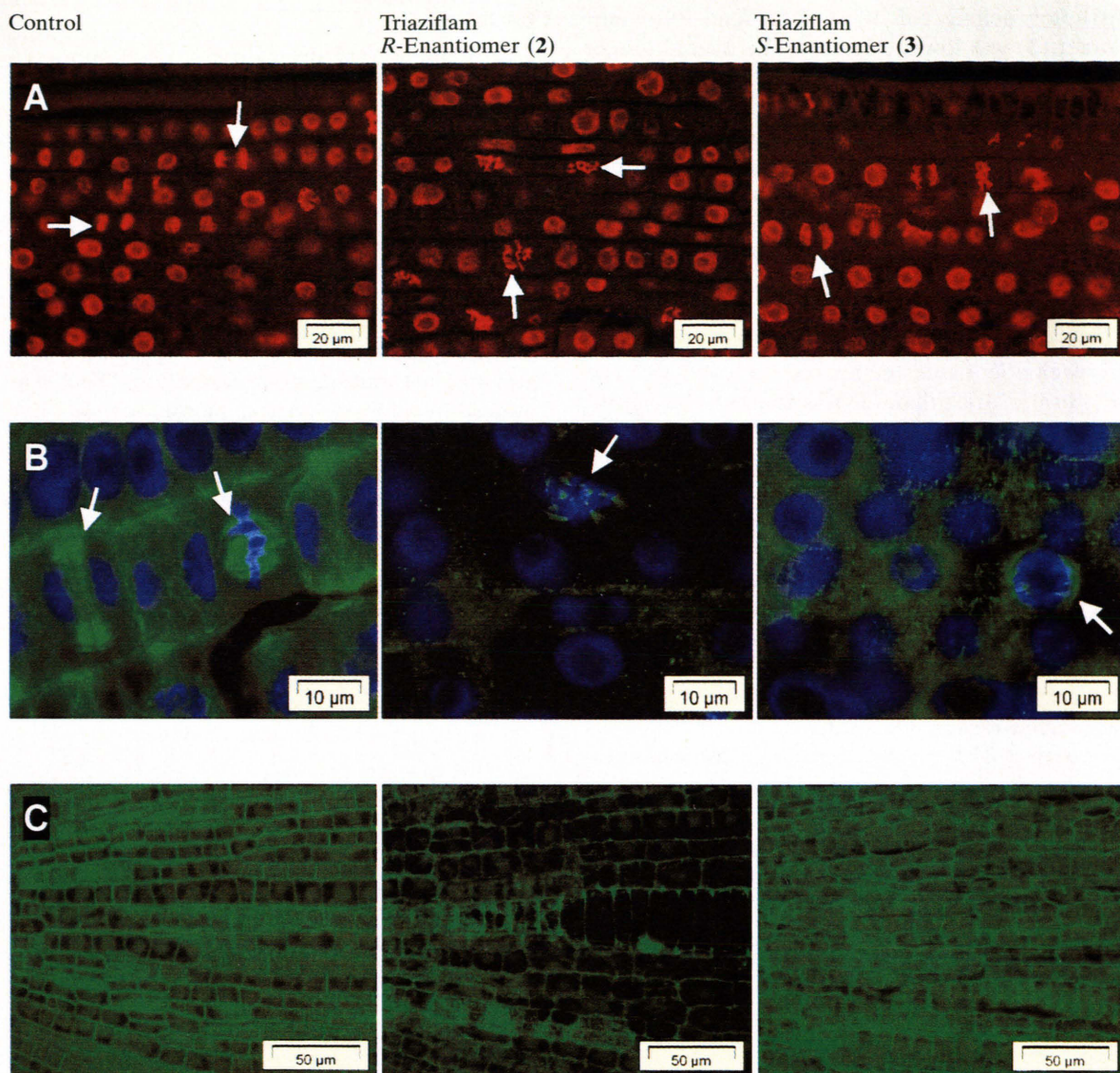


Fig. 5. Effects of triaziflam enantiomers (**2**, **3**) on mitosis, the microtubule cytoskeleton and deposition of cellulose in cell walls of meristematic maize root cells. Maize seedlings were treated with 10  $\mu\text{M}$  of compounds for 4 and 24 h hydroponically. Tips of primary and adventitious roots were sampled and serial longitudinal sections were processed for fluorescence microscopic examination. A, Feulgen staining of mitotic structures, 4 h after treatment. Control root tip cells undergoing mitosis. Triaziflam-(*R*)-treated cells in arrested prometaphase, triaziflam-(*S*)-treated cells showing few cells at later mitotic stages (denoted by arrows). B, Immunofluorescent staining of microtubules, 4 h after treatment. Control cells showing cortical, spindle and phragmoplast microtubules (denoted by arrows). Triaziflam-(*R*)-treated cells showing a decrease in cortical and a complete loss in preprophase, spindle and phragmoplast microtubules. Kinetochore tufts of microtubules are still visible (denoted by arrow). Triaziflam-(*S*)-treated cells showing cortical and preprophase band microtubules (denoted by arrow). C, Fluorescent staining of cellulose using a cellulose-binding domain, 24 h after treatment. Control cells showing cellulose deposition in cell walls. Decrease of cellulose deposition in cell walls after treatment particularly with triaziflam-(*R*)-enantiomer.



disrupter activity of 10  $\mu\text{M}$  triaziflam (*S*)-enantiomer (**3**) was lower (Fig. 5B). The overall loss of microtubules was less pronounced.

Deposition of cellulose microfibrils in cell wall formation was studied using an isolated bacterial cellulose-binding domain conjugated to a fluorescent dye. Cellulose localization was conducted after enzymatic digestion of hemicelluloses and pectins in sections of maize root tips. As shown in the micrographs (Fig. 5C), treatment of maize roots with 10  $\mu\text{M}$  of the (*R*)-form of triaziflam (**2**) for 24 h reduced staining for cellulose in cell walls of meristematic tissue, compared to controls. The (*R*)-form of triaziflam (**2**) was found to be significantly more active than the (*S*)-form (**3**; Fig. 5C). After treatment for 4 h, both enantiomers caused only slight changes (not shown). The cellulose microfibrils appeared to be randomly oriented in the cell walls particularly after exposure to triaziflam (*R*)-enantiomer (**2**). This points to an indirect effect of triaziflam derived from microtubule disruption, because the orientation of newly deposited cellulose microfibrils are determined by cortical microtubules (Vaughn 2000). However, the decrease in cellulose deposition in cell walls found after 24 h of treatment indicates inhibition of cellulose synthesis by triaziflam. This is in accordance with recent studies by K. Kreuz (Syngenta Crop Protection AG, Basel; based on a paper presented at a symposium held at Uni. Marburg, Germany, on 6<sup>th</sup> November 2000).

## Conclusion

Triaziflam and the derivatives studied, showed a dual, enantioselective mode of action, which is based on (1) PET inhibitory activity under light conditions and (2) non-light-dependent effects on seedling and cell suspension growth. Taken together, the symptoms induced on dark-grown seedlings and the histochemical observations described above showed that triaziflam blocks cell division enantioselectively – with the (*R*)-form (**2**) as the most active isomer. The herbicide caused disruption of mitosis by inhibiting spindle and phragmoplast microtubule formation. This was followed by a loss of cortical microtubules leading to the production of isodiametric cell growth. The symptomatology of mitotic disruption resembles that caused by herbicides from the carbamate (e.g. propyzamide)- or dinitroaniline (e.g. pendimethalin)-type, but in comparison to the latter, the efficacy of triaziflam is lower. As a secondary effect induced later after treatment, cellulose synthesis in cell wall formation appeared to be affected. This could additionally promote the formation of isodiametric cells and consequently root swelling and could further lead to cellular damage.

## Acknowledgements

The authors thank Sigrid Hennig, Simone Huber and Anneliese Keller for technical assistance and Dr. Rex Liebl (BASF, Limburgerhof, Germany) for critical reading of the manuscript and valuable discussion.

- Avron M. and Shavit N. (1963), A simple method for determination of ferrocyanide. *Anal. Biochem.* **6**, 549–554.
- Backer H. J. and Wanmaker W. L. (1951), Trichloracétamidines substitués. *Recueil Trav. Chim. Pays-Bas* **70**, 638–644.
- Cross B. and Feeny R. W. (1974), Substituted *s*-triazines as herbicidal agents. Patent US 3816419.
- Eun S.-O., Youn, H. S. and Lee Y. (2000), Lead disturbs microtubule organization in the root meristem of *Zea mays*. *Physiol. Plant.* **110**, 357–365.
- Fuerst E. and Norman M. A. (1991), Interactions of herbicides with photosynthetic electron transport. *Weed Sci.* **39**, 458–464.
- Grossmann K. and Retzlaff G. (1997), Bioregulatory effects of the fungicidal strobilurin kresoxim-methyl in wheat (*Triticum aestivum*). *Pestic. Sci.* **50**, 11–20.
- Grossmann K., Berghaus R. and Retzlaff G. (1992), Heterotrophic plant cell suspension cultures for monitoring biological activity in agrochemical research. Comparison with screens using algae, germinating seeds and whole plants. *Pestic. Sci.* **35**, 283–289.
- Masahiro N., Kobayashi I., Uemura M. and Takematsu T. (1990), Triazine derivative and herbicide containing the same as active ingredient. Patent EP 411153.
- Münster P., Freund W., Maywald V., Kükenhöfner T., Gerber M., Grossmann K. and Walter H. (1995), Synthesis and herbicidal activity of isoxazoledicarboxylic acid derivatives. *Pestic. Sci.* **44**, 21–27.
- Omokawa H. and Konnai M. (1992), Inhibition of *Echinochloa crus-galli* var. frumentacea seedling root elongation by chiral 1,3,5-triazines in the dark. *Pestic. Sci.* **35**, 83–86.
- Omokawa H., Ichizen N. and Takematsu T. (1987), Phytotoxic properties of *a*-substituted benzylamino-*s*-triazines. *Agric. Biol. Chem.* **51**, 2563–2568.
- Omokawa H., Kuramochi H., Kawata Y. and Konnai M. (1994), Structural characteristics of *s*-triazine compounds inducing rhizome in *Cyperus serotinus* Rottb. *J. Pesticide Sci.* **19**, 25–32.
- Riebel H.-J., Lehr S., Stelzer U., Watanabe Y., Dollinger M., Dahmen P., Seishi I., Goto T. and , Yanagi A. (1998), Preparation of 2-amino-4-alkylamino-1,3,5-triazines as herbicides. Patent WO 98/15539.
- Ruzin S. E. ed. (1999), *Plant Microtechnique and Microscopy*. Oxford University Press, Oxford.
- Taylor J. G., Haigler C., Kilburn D. G. and Blanton R. L. (1996), Detection of cellulose with improved specificity using laser-based instruments. *Biotechnic and Histochemistry* **71**, 215–223.
- Vaughn K. C. (2000), Anticytoskeletal herbicides. In: *Plant Microtubules. Potential for Biotechnology* (P. Nick, ed.). Springer, Berlin, Heidelberg, pp.193–205.